1336 *Biochemistry* **2011,** *50,* 1336–1346
DOI: 10.1021/bi101734q

BIOCHEMISTRY
including biophysical chemistry & molecular biology
Article

In Vitro Hybridization and Separation of Hybrids of Human Adenylosuccinate Lyase from Wild-Type and Disease-Associated Mutant Enzymes[†]

Lushanti De Zoysa Ariyananda, Christina Antonopoulos, Jenna Currier, and Roberta F. Colman*

Department of Chemistry and Biochemistry, University of Delaware, Newark, Delaware 19716, United States

Received October 28, 2010; Revised Manuscript Received January 6, 2011

ABSTRACT: Human adenylosuccinate lyase (ASL) deficiency is an inherited metabolic disease in which the majority of the patients are compound heterozygotes for the mutations that occur in the ASL gene. Starting with purified wild-type (WT) and single-mutant human ASL, we generated in vitro hybrids that mimic compound heterozygote ASL. For this study, we used His-tagged WT/non-His-tagged WT, His-tagged WT/non-His-tagged R396C, His-tagged WT/non-His-tagged R396H, His-tagged R194C/non-His-tagged R396C, and His-tagged L311V/non-His-tagged R396H enzyme pairs. We generated various hybrids by denaturing pairs of enzymes in 1 M guanidinium chloride and renaturing them by removing the denaturant. The hybrids were separated on a nickel−nitrilotriacetic acid−agarose column based on the number of His tags present in the enzyme tetramer. Analytical ultracentrifuge data indicate that the hybrids have predominant amounts of heterotetramers. Analysis of the V_{max} values of the hybrids indicates that most of the subunits behave independently; however, the hybrid tetramers retain weak positive cooperativity, indicating that there is some interaction between the different subunit types. The interactions between WT and mutant subunits may be advantageous to the parents of ASL deficient patients, while the interactions between some mutant subunits may assist heterozygote ASL deficient patients.

Adenylosuccinate lyase (ASL)[1] is an important enzyme (EC 4.3.2.2) in the de novo purine biosynthesis pathway and the purine nucleotide cycle (*1*). The reactions catalyzed by ASL are shown in Figure 1. Mutations in the adenylosuccinate lyase gene (the majority of which are missense mutations) lead to adenylosuccinate lyase deficiency, which is associated with mental retardation and autism. In these cases, the accumulation of succinyl adenosine (S-Ado) and succinyl aminoimidazole carboxamide riboside (SAICAr) (the dephosphorylated products of ASL substrates) in the cerebrospinal fluid, plasma, and urine is used to diagnose ASL deficiency (*2*−*4*). We have previously studied five purified disease-associated human mutant ASLs, each of which has a single mutation: R194C, L311V, R396C, R396H, and K246E (*5*). The specific activities of the first two mutants are similar to that of wild-type ASL, while the specific activities of R396C, R396H, and K246E are considerably lower; all of the mutants exhibit decreased kinetic cooperativity (*5*).

Most of the ASL deficient human patients are compound heterozygotes, in which each gene carries a mutation inherited from one parent. Often, these disease-associated point mutations occur at different regions of the enzyme far from the active site (*6*, *7*). Two such compound heterozygous combinations that are present in two different patients are R194C/R396C and L311V/R396H (*2*, *8*). The patient with the R194C/R396C combination was a boy with a neonatal fatal form of ASL deficiency, which is characterized by neonatal microcephaly, cerebral atrophy, hyperkinesis, and an extremely low body weight percentile (*2*). The boy died at the age of 6 weeks. In contrast, the patient with the L311V/R396H combination was a girl with a severe childhood form of ASL deficiency, which developed after the first month of life and progressed slowly with age, ultimately resulting in severe mental retardation accompanied by white matter degeneration in the brain, muscle wasting, and autistic features (*8*). At the time of the report, the girl was 6 years of age. As indicated in the two reports, both patients had very low levels of adenylosuccinate lyase activity (*2*, *8*).

Adenylosuccinate lyase is a homotetramer, each active site consisting of different regions of three subunits (Figure 2, I) (*9*). For *Bacillus subtilis* ASL, it has been demonstrated that in vitro mixing of two inactive mutant enzymes with replacements for different amino acids can lead to intersubunit complementation with a partial restoration of activity (*10*−*12*). Accordingly, we have hypothesized that in human compound heterozygote patients intersubunit complementation may occur, which may be advantageous to the patient as compared to homozygote patients. As shown in panels II and III of Figure 2, in compound heterozygote patients only one type of mutation is present in each subunit; it is postulated that in some of the enzyme species if the R194C mutation is present in one subunit, the R396C mutation may be present in the adjacent subunit or if the L311V mutation occurs in one subunit, the R396H mutation may be located on the

[†]This work was supported by National Institutes of Health (NIH) Grant R01-DK60504 and by a grant from Autism Speaks. The Beckman Optima XL-I analytical ultracentrifuge used in this study was obtained and supported by NIH Grant 2P20 RR016472.

*To whom correspondence should be addressed. Telephone: (302) 831-2973. Fax: (302) 831-6335. E-mail: rfcolman@udel.edu.

[1]Abbreviations: ASL, adenylosuccinate lyase; S-Ado, succinyl adenosine; SAICAr, succinyl aminoimidazole carboxamide riboside; SAICAR, 5-aminoimidazole-4-(*N*-succinylocarboxamide ribonucleotide); AICAR, 5-aminoimidazole-4-carboxamide ribonucleotide; SAMP, adenylosuccinate; Ni−NTA, nickel−nitrilotriacetic acid−agarose; SDS-PAGE, sodium dodecyl sulfate−polyacrylamide gel electrophoresis; MOPS, 3-(*N*-morpholino)propanesulfonic acid; LDS, lithium dodecyl sulfate; AUC, analytical ultracentrifugation; HEPES, *N*-(2-hydroxyethyl)piperazine-*N*′-2-ethanesulfonic acid; PDB, Protein Data Bank.

 Published on Web 01/06/2011

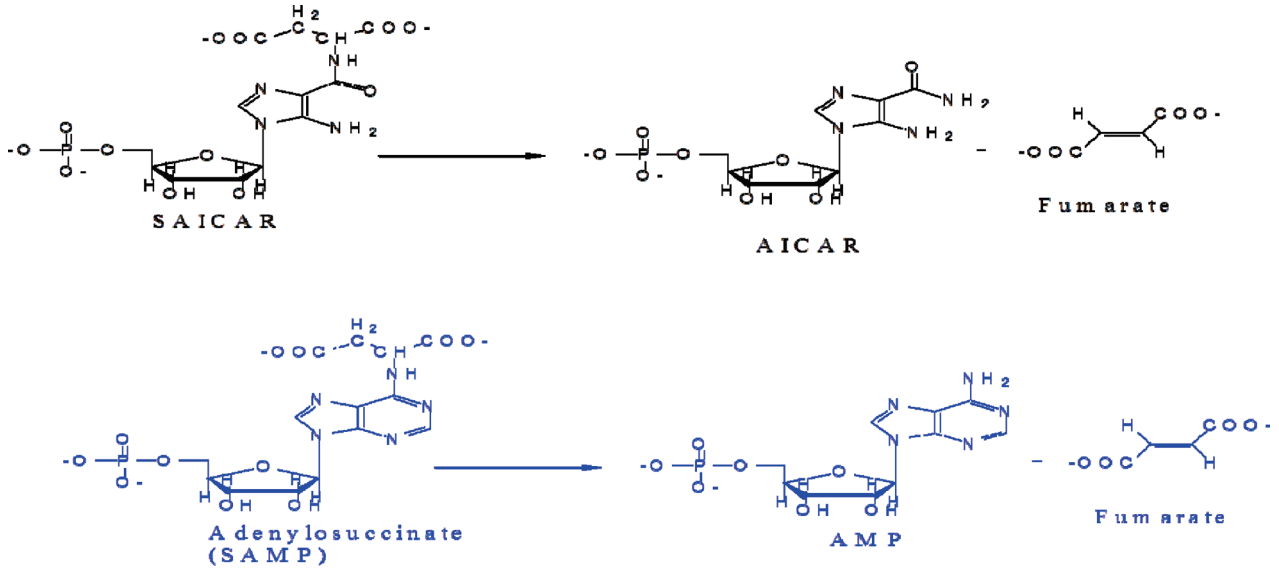

FIGURE 1: Schematic representations of reactions catalyzed by adenylosuccinate lyase: (top) cleavage of SAICAR to AICAR and fumarate and (bottom) cleavage of SAMP to AMP and fumarate.

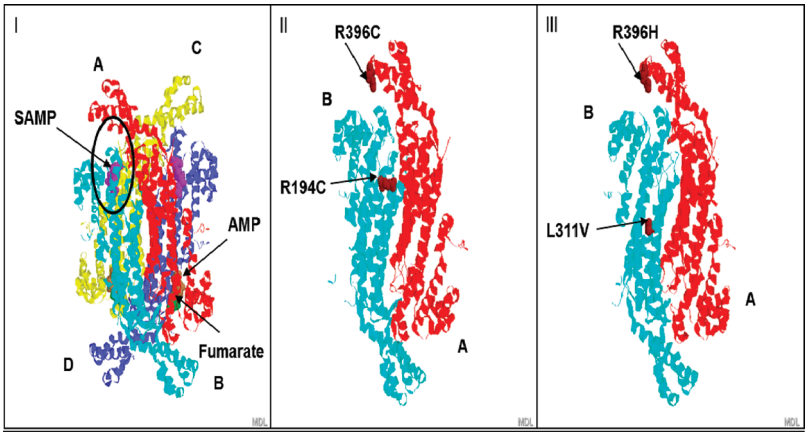

FIGURE 2: Representation of the mutated subunits in compound heterozygote human ASL deficient patients. (I) Crystal structure of the human ASL, which was crystallized with the products (AMP and fumarate) and substrate (SAMP) (PDB entry 2VD6) (*14*). Each individual subunit is color-coded, and one active site of four is designated by a circle. Panels II and III show the compound heterozygote R194C/R396C and L311V/R396H pairs, respectively, in which each mutation is present in only one subunit.

adjacent subunit. This hypothesis has not yet been critically evaluated. Therefore, this study focuses on in vitro hybridization using the wild type and four purified mutant proteins, and separation and characterization of hybrid mutant proteins in the cases of the R194C/R396C and L311V/R396H pairs. A preliminary version of this work has been presented (*13*).

EXPERIMENTAL PROCEDURES

Materials. SAMP, HEPES, imidazole, and Sephadex (G-100) were purchased from Sigma Chemicals. Nickel−nitrilotriacetic acid−agarose (Ni−NTA) was obtained from QIAGEN. Precast NuPAGE Bis-Tris 4−12% gels, NuPAGE MOPS SDS running buffer (pH 7.7), LDS sample buffer, antioxidant, and reducing agent were obtained from Invitrogen. Human α-thrombin was from Enzyme Research Laboratories. The silver stain kit was purchased from Pierce Inc. All other reagents were from Fisher Scientific and were of reagent grade. SAICAR was prepared enzymatically from AICAR and fumarate by S. Sivendran as described in ref *15*.

Site-Directed Mutagenesis, Enzyme Expression, and Purification. We have previously described site-directed mutagenesis and the introduction of mutations (R194C, L311V, R396H, and R396C) into the pETN25HASL plasmid (*5*). The human wild-type (WT) and mutant ASLs were expressed as N-terminal His_6-tagged proteins in the *Escherichia coli* Rosetta 2 (DE3) (pLysS) strain.

The WT and mutant enzymes were purified to homogeneity using chromatography on Qiagen Ni−NTA (*16*). The purity of the enzymes was assessed electrophoretically at pH 8.6 using 12% polyacrylamide gels containing 0.1% sodium dodecyl sulfate (*17*). The protein concentration of human ASL was determined by the absorbance at 280 nm using an $E_{280}^{1\%}$ of 14.1 (*18*). After purification, each enzyme was aliquoted and stored at −80 °C in 50 mM potassium phosphate buffer (pH 7.0) containing 150 mM KCl, 1 mM EDTA, 1 mM DTT, and 10% glycerol (enzyme storage buffer). Frozen enzyme samples were preincubated at 25 °C for ~1 h prior to any experiment because it has been shown both for the *B. subtilis* ASL (*19*) and for the human ASL (*16*) that the restoration of full activity is a slow process.

The specific activity of the purified protein was measured continuously by assaying in 1 mL (over a 1 min period) at 25 °C using 60 μM SAMP in 50 mM HEPES buffer (pH 7.4) (standard assay). The activity was measured from the decrease in absorbance at 282 nm as SAMP is converted to AMP and fumarate. The difference extinction coefficient of 10000 M^{-1} cm^{-1} between SAMP and AMP was used to calculate the specific activity, which was expressed in micromoles of substrate converted per minute per milligram of enzyme used (*20*).

The specific activity of ASL with respect to SAICAR was measured continuously by assaying in 1 mL (over a 1 min period) at 25 °C using 60 μM SAICAR in 50 mM HEPES buffer (pH 7.4). The activity was measured from the decrease in absorbance at 269 nm as SAICAR is converted to AICAR and fumarate. The difference extinction coefficient of 700 M^{-1} cm^{-1} between SAICAR and AICAR was used to calculate the specific activity, which was expressed in micromoles of substrate converted per minute per milligram of enzyme used (*21*).

Removal of the Six-Histidine Tag from the WT and Mutant Enzymes. The recombinant human ASL was constructed to have a six-His tag and a thrombin cleavage site before the actual protein sequence. The amino acid sequence of the additional part is MGSSHHHHHHSSGLVPRGSH, and the thrombin cleaves between arginine and glycine of this sequence. The molecular masses of the His-tagged protein, the non-His-tagged protein, and the cleaved peptide portion are ~57000, ~55000, and ~1700 Da, respectively. To remove DTT and change the pH, we first dialyzed the ASL sample overnight against 50 mM potassium phosphate buffer (pH 8) containing 300 mM potassium chloride and 10% glycerol. Subsequently, an appropriate amount of thrombin (10 units of thrombin/mg of ASL) was added to the enzyme sample, which was then incubated at 25 °C for ~24 h. To separate the His-tagged peptide from the non-His-tagged protein, we loaded the mixture on a Sephadex G-100 column (50 mL), which was equilibrated with the enzyme storage buffer (pH 7.0). DTT (1 mM) was added to the enzyme sample before it was loaded on the column to stabilize ASL and inactivate the thrombin. The fractions (1 mL) were eluted using enzyme storage buffer (pH 7.0), and the activity of each fraction was recorded. The fractions with the highest activity were pooled and concentrated. The presence of a pure non-His-tagged protein was confirmed by either N-terminal sequencing or mass spectroscopy. We have previously demonstrated that His-tagged and non-His-tagged human ASL exhibit similar specific activities and kinetic parameters (*16*).

Dependence of Denaturation and Renaturation of WT ASL on the Concentration on Guanidinium Chloride. The preincubated WT enzyme sample (6 mg) was dialyzed overnight against enzyme storage buffer (pH 7.0) that has no glycerol (buffer B). The concentration and the activity of the enzyme sample were measured after dialysis. For each experiment, 1 mg of wild-type enzyme was used. The WT enzyme in buffer B (pH 7.0) containing various concentrations of guanidinium chloride (0.5−3 M) was separately incubated at 25 °C for 1 min. During the incubation, aliquots were withdrawn and assayed at 25 °C, by addition of a 5 μL aliquot of enzyme to 1.0 mL of solution containing 50 mM HEPES (pH 7.4), 60 μM SAMP, and guanidinium chloride, to yield each concentration that was used for the incubation. After the 1 min incubation period, the enzyme sample was diluted 5-fold with 50 mM potassium phosphate buffer (pH 7.0) containing 150 mM KCl, 0.1 mM DTT, and 10% glycerol (nickel column buffer), and the diluted mixture was incubated at 25 °C to restore activity. At regular time intervals, aliquots were withdrawn and assayed under standard assay conditions to determine the percentage of activity regained.

Denaturation and Renaturation of Mutant Enzymes with Guanidinium Chloride. The WT and mutant enzyme samples were preincubated at 25 °C for ~1 h, and each sample was diluted with enzyme storage buffer (pH 7.0) lacking glycerol to yield a concentration of 2 mg/mL. To each enzyme sample was added guanidinium chloride to yield a final concentration of 1 M, and the enzyme samples were incubated at room temperature for 30 s. During the incubation, an aliquot from each enzyme sample was withdrawn and assayed at 25 °C, by addition of a 5 μL aliquot of enzyme to 1.0 mL of solution containing 50 mM HEPES (pH 7.4), 60 μM SAMP, and guanidinium chloride, to yield a final concentration of 1 M. Subsequently, each mixture was diluted 5-fold with nickel column buffer (pH 7.0) and dialyzed against the same buffer for 1 h to lower the guanidinium concentration and allow renaturation. The fluorescence intensities of mutant enzymes in fresh nickel column buffer (pH 7.0) were measured on a Perkin-Elmer MPF-3 fluorescence spectrophotometer, which was thermostated at 25 °C. The enzyme solutions were excited at 290 nm, which is specific for tryptophan residues. The emission intensity of each enzyme sample before and after the guanidine treatment was recorded at 335 nm.

Standardization of the Ni−NTA Column Using His-Tagged and Non-His-Tagged WT Human ASL. A mixture containing equal amounts (2 mg of each) of the His-tagged WT and non-His-tagged WT enzymes that was not treated with guanidinium chloride was loaded onto 1 mL of the Qiagen Ni−NTA column equilibrated with nickel column buffer (pH 7.0). A total volume of 2 mL was loaded onto the column, which was first washed with 100 mL of nickel column buffer (pH 7.0). Subsequently, a linear gradient of imidazole (from 0 to 250 mM) was used (formed from 100 mL of starting buffer and 100 mL of starting buffer containing 250 mM imidazole), and 2.5 mL fractions were collected in tubes containing 250 μL of enzyme storage buffer (pH 7.0) containing 10 mM DTT. The absorbance of each fraction at 280 nm was recorded, and the blank absorbance of each fraction at 280 nm was subtracted to yield the elution profile. To obtain the absorbance of the blank, we passed a linear gradient of imidazole (from 0 to 250 mM) through the column that had no bound enzyme. Fractions of 2.5 mL were collected in the tubes containing 250 μL of enzyme storage buffer (pH 7.0) containing 10 mM DTT. The collected wash flow-through and the fractions with high absorbance were concentrated to 1 mL using an Amicon ultracentrifugation unit, which has a molecular weight cutoff of 10000. The absorbance at 280 nm and enzymatic activity of each pool were measured.

In Vitro Hybridization of WT and Mutant Enzymes and Separation of the Hybrids. The in vitro hybridization and separation of hybrids were performed as described below using the following pairs of enzymes: His-tagged WT/non-His-tagged WT, His-tagged WT/non-His-tagged R396C, His-tagged WT/non-His-tagged R396H, His-tagged L311V/non-His-tagged R396H, and His-tagged R194C/non-His-tagged R396C.

For each hybridization reaction, a mixture (2 mL) was prepared from the two preincubated enzyme samples (2.5 mg of each enzyme) and guanidinium chloride, yielding a final concentration of 1 M, and enzyme storage buffer (pH 7.0) that has no glycerol. The mixture was incubated at 25 °C for 20−30 s. During the incubation, an aliquot was withdrawn and assayed in the presence of 1 M guanidinium chloride as described above.

Subsequently, the mixture was diluted 5-fold using nickel column buffer (pH 7.0) and dialyzed against the same buffer, for 1 h to lower the guanidine concentration and allow renaturation. The mixture was removed from the buffer and centrifuged at 10000 rpm and 25 °C for ~1 min to remove any precipitate. The clear supernatant was loaded onto a 1 mL column of Qiagen Ni−NTA, which was equilibrated with nickel column buffer (pH 7.0). The column was first washed using 100 mL of nickel column buffer (pH 7.0). Then a linear gradient of imidazole (from 0 to 250 mM) was passed through the column, and fractions (2.5 mL) were collected in tubes containing 250 μL of enzyme storage buffer (pH 7.0) with 10 mM DTT. A total volume of 200 mL of gradient was used for the separation. The absorbance at 280 nm was measured in each fraction, and each peak was pooled. The wash flow-through and each pool were concentrated to 1 mL by centrifugation at 5000 rpm using an Amicon ultracentrifugation unit, which has a molecular weight cutoff of 10000. To lower the imidazole concentration, we added ~15 mL of enzyme storage buffer (pH 7.0) to the Amicon ultracentrifugation unit, which had 1 mL of concentrated fraction, and centrifuged the mixture at 5000 rpm to concentrate it to 1 mL. This process was repeated three times for each pool. The pools were kept at 25 °C for ~3 days after being eluted from the column. The kinetics, gels, and analytical ultracentrifugation (AUC) were conducted within 2−3 days of eluting the fractions. Any remaining pools were aliquoted and stored at −80 °C.

Thermal Stability at 60 °C. The pool 2 enzyme samples (0.2 mg/mL) of all the hybrid pairs in fresh enzyme storage buffer (pH 7.0) were incubated at the harsh temperature of 60 °C. Aliquots were removed periodically and assayed for 1 min under standard assay conditions at 25 °C. All the enzyme samples were pre-incubated at 25 °C for ~1 h before being heated to 60 °C for stability measurements. The k_i value for each reaction was determined from the slope of $\ln(E_t/E_0)$ versus time.

Determination of Subunit Ratios by SDS−PAGE. The precast 4−12% Bis-Tris acrylamide gels from Invitrogen were used to perform SDS−PAGE. The samples for the SDS gels were prepared according to the manufacturer's protocol using the standards (His-tagged and non-His-tagged enzymes of each pair) and each pool of 0.1 mg/mL. Each sample (2 μL) was loaded onto the gel, and electrophoresis was performed at 200 V for 2 h using SDS-MOPS running buffer. The gels were stained using the silver stain kit (Pierce Inc.) according to the manufacturer's protocol. The stained gels were scanned, and the area of each band was measured using ImageJ (*22*). Each sample was repeated two or three times.

Kinetics of Hybrid Pools. The activities of the different pools of enzyme hybrids in fresh enzyme storage buffer (pH 7.0) were measured by assaying for 1 min under standard assay conditions. The kinetic parameters were determined by varying the SAMP concentrations (0.2−10 μM). Because the data did not obey simple Michaelis−Menten kinetics, they were analyzed using the Hill equation, $v = (V_{max}[S]^n)/([S]^n + K_{0.5})$, where n is the Hill coefficient and $K_{0.5}$ is the substrate concentration yielding half the V_{max}. The standard error estimates were obtained from SigmaPlot (SPSS Inc., Chicago, IL).

Molecular Mass Determination Using Analytical Ultracentrifugation. To assess the species present in each pool, sedimentation equilibrium (SE) was used. SE experiments with the WT and mutant enzymes were conducted using a Beckman Coulter ProteomLab XL-I analytical ultracentrifuge equipped with an An-60Ti analytical rotor and six-chamber centerpiece assembly. Each sample was loaded in duplicate or triplicate into each six-chamber centerpiece. Samples (~0.1 mg/mL) were centrifuged at 11000 rpm and 25 °C. Some of the pure mutant samples (R194C, R396C, and L311V) were also centrifuged at 9000 rpm and 25 °C. Because the results were similar at 9000 and 11000 rpm, the comparison was conducted at 11000 rpm. After equilibrium had been reached (~20 h), stepwise radial scans were performed at 280, 240, and 220 nm, using a step size of 0.001 cm (*23*). Initially, the equilibrium time was determined by scanning at 5 h intervals for ~20 h. The species present in each pool was evaluated by analyzing the data using the noninteracting discrete species model in SEDPHAT (*24*), which assumes that there is no interaction among the species during the time of the SE experiment. In all cases, the experimental data were fitted to all the possible theoretical models of an oligomer with species with lower molecular masses. The models that gave best fits were chosen as being representative of that sample. The density of the buffer at 25 °C was calculated using SEDNTERP (*25*). The partial specific volume of human ASL at 25 °C is 0.73698. We have used a similar approach previously in analyzing the molecular mass of WT and mutant *B. subtilis* and human ASL (*5*, *26*).

RESULTS

Expression and Purity of the Human ASL WT and Mutants. Wild-type and mutant enzymes were expressed and purified to homogeneity by the methods described previously (*16*), and the purity was assessed using SDS−PAGE and mass spectroscopy. Each His-tagged and non-His-tagged enzyme exhibited a single subunit band via SDS−PAGE (*5*). The mass analysis of each of the enzymes indicated that the molecular masses of His-tagged and non-His-tagged enzymes are ~57000 and ~55000 Da, respectively.

Denaturation and Renaturation of WT and Mutant Human ASL. To perform in vitro protein hybridization, it is desirable that the two enzymes dissociate to subunits in the presence of a denaturant and then reassociate to form a tetramer with minimal conformational changes upon removal of the denaturant. If there are two different subunit types present in the denaturant solution, various heterotetramers can be formed as the denaturant is removed. We chose guanidinium chloride as the denaturant and, as a screen for conditions, sought to evaluate the concentration dependence of inactivation of human WT ASL by guanidinium chloride. Because glycerol stabilizes proteins, the WT enzyme was dialyzed overnight to remove glycerol prior to the experiment. As represented in Figure 3, during the 1 min incubation of human WT ASL in the presence of ≥1 M guanidinium chloride, there is complete loss of activity. When the guanidinium chloride is diluted 5-fold, the activity is restored to various extents (Figure 3). However, some of the mutant enzymes were unstable in the presence of ≥1.5 M guanidinium chloride under the same denaturation and renaturation conditions. In contrast, all the mutant enzymes were equally stable when they were diluted directly with enzyme storage buffer (pH 7.0) lacking glycerol immediately prior to the guanidine treatment followed by denaturation (in the presence of 1.0 M guanidinium chloride for 30 s) and renaturation. This is the procedure that was followed subsequently.

The activity and fluorescence emission intensity (which is an indication of the enzyme's conformational state) of each sample were measured before and after the guanidinium chloride treatment,

and the results are listed in Table 1. It is evident that the enzymes regained full activity when the mixture was diluted 5-fold and dialyzed for 1 h to lower the guanidinium chloride concentration and allow renaturation. Furthermore, there is minimal change in emission fluorescence intensity upon comparison of each sample before and after the guanidinium chloride treatment, indicating that denaturation is reversible and does not cause major conformational changes in any of the enzymes.

In Vitro Hybridization and Separation of Hybrids. In vitro hybridization was conducted by mixing equal amounts of the appropriate non-His-tagged and His-tagged enzyme pairs as described in Experimental Procedures. Because human ASL is a tetramer, three different types of hybrid tetramers with non-His-tagged:His-tagged ratios of 3:1, 2:2, and 1:3 can form during hybridization, as well as the 4:0 and 0:4 tetramers of the original His-tagged and non-His-tagged proteins. Separation of the mixture was accomplished by using a nickel column; affinity for the column depends on the number of His tags present on the tetramer. Theoretically, the non-His-tagged protein should elute first, and several hybrids should be separated by the imidazole gradient as follows: earliest should be the 3:1 mixture (non-His-tagged:His-tagged), followed by the 2:2 mixture, and then the 1:3 mixture, and last should be the pure His-tagged protein.

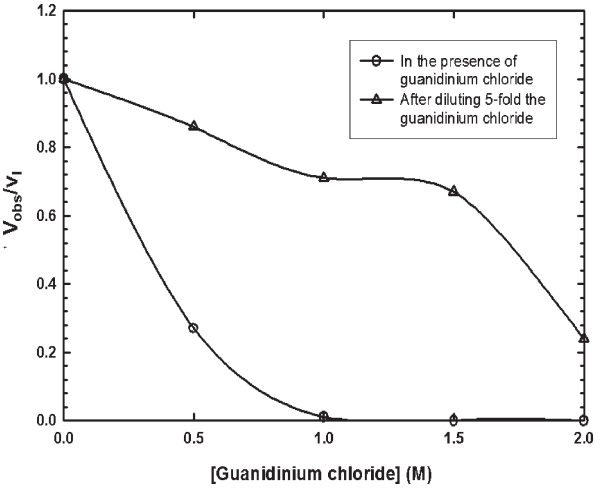

FIGURE 3: Fraction of specific activity of human WT ASL at 25 °C in the presence of different concentrations of guanidinium chloride (○) and after 5-fold dilution of the guanidinium chloride (△). v_i and v_{obs} are the specific activities of the enzyme without guanidinium chloride and during the denaturing and renaturing process, respectively.

The 1.0 mL nickel column was standardized using a mixture of an equal amount of His-tagged WT and non-His-tagged WT enzyme that had not undergone the guanidinium chloride treatment. Once the mixture had been loaded onto the column, it was washed with nickel column buffer (pH 7.0) that lacks imidazole. No ASL activity was detected in the wash fraction after concentration, implying that even the non-His-tagged WT enzyme binds to the nickel column. In the imidazole gradient, the non-His-tagged WT enzyme elutes between 12 and 40 mL with a maximum at ~20 mL, while the pure His-tagged enzyme elutes between 130 and 175 mL with a maximum at ~140 mL (Figure 4). Absorbance and ASL activity were not detected between effluent volumes of 40 and 130 mL, suggesting that hybridization does not occurr without the guanidinium treatment. Furthermore, these results indicate that there is a relatively large distinction between the pure non-His-tagged and His-tagged protein, which allows good separation of the hybrids.

To assess the feasibility of the hybridization protocol, we used a mixture of His-tagged WT and non-His-tagged WT enzymes to perform the in vitro hybridization and separation of the hybrids. Because R396H and R396C mutant enzymes have very low (~20% of WT activity) activity, we sought to evaluate whether high-activity hybrids are formed between WT and the R396C and -H mutants. This scenario mimics the situation for parents of the ASL deficient patients, as each parent has only one mutation in one gene while the other gene corresponds to the WT protein. To mimic the human ASL deficient patients, appropriate enzyme pairs (R194C/R396C and L311V/R396H) were used to perform the in vitro hybridization. The elution profiles of His-tagged WT/non-His-tagged WT, His-tagged WT/non-His-tagged R396C, and His-tagged R194C/non-His-tagged R396C pairs in the presence of the imidazole gradient are shown in Figure 4A. The elution profiles of His-tagged WT/non-His-tagged WT, His-tagged WT/non-His-tagged R396H, and His-tagged L311V/non-His-tagged R396H pairs in the presence of the imidazole gradient are shown in Figure 4B. The peak positions of pure non-His-tagged WT ASL and pure His-tagged WT ASL are indicated above the graph.

The elution profiles of all the enzyme pairs show four peaks compared to the two peaks of the mixture of His-tagged WT and non-His-tagged WT enzymes without the guanidinium treatment. Hence, the two middle pools, pools 2 and 3, contain different types of hybrid mixtures. The amount of hybrid in the final preparations is represented by the areas under peaks 2 and 3 as compared to the total area under peaks 1−4. We estimate that

Table 1: Activities and Fluorescence Intensities of WT and Mutant Human ASL at 25 °C before and after Guanidinium Chloride (Gdn.HCl) Treatment

	before Gdn.HCl treatment		after Gdn.HCl treatment[a]	
enzyme	specific activity[b] (μmol min^{-1} mg^{-1})	fluorescence intensity at 335 nm[c]	specific activity[b] (μmol min^{-1} mg^{-1})	fluorescence intensity at 335 nm[c]
His-tagged WT	8.5 ± 0.2	41 ± 1.0	8.3 ± 0.1	42 ± 0.5
non-His-tagged WT	8.6 ± 0.1	42 ± 0.5	8.4 ± 0.2	42 ± 1.0
His-tagged L311V	7.8 ± 0.2	36 ± 1.0	7.5 ± 0.1	37 ± 0.5
non-His-tagged R396H	1.0 ± 0.2	44 ± 1.0	1.1 ± 0.1	43 ± 0.5
His-tagged R194C	8.7 ± 0.2	42 ± 0.5	8.9 ± 0.2	41 ± 0.5
non-His-tagged R396C	1.8 ± 0.1	41 ± 1.0	1.6 ± 0.2	40 ± 0.5

[a]Each enzyme (2 mg/mL) was incubated at 25 °C in the presence of 1 M guanidinium chloride for 30 s and diluted 5-fold followed by dialysis for 1 h at room temperature. [b]The specific activity of each enzyme sample was measured continuously by assaying (over a 1 min period) at 282 nm using 60 μM SAMP in 50 mM HEPES buffer (pH 7.4) at 25 °C. [c]The fluorescence emission intensity of each enzyme sample was measured at 335 nm, and the intensities were normalized to a protein concentration of 0.33 mg/mL.

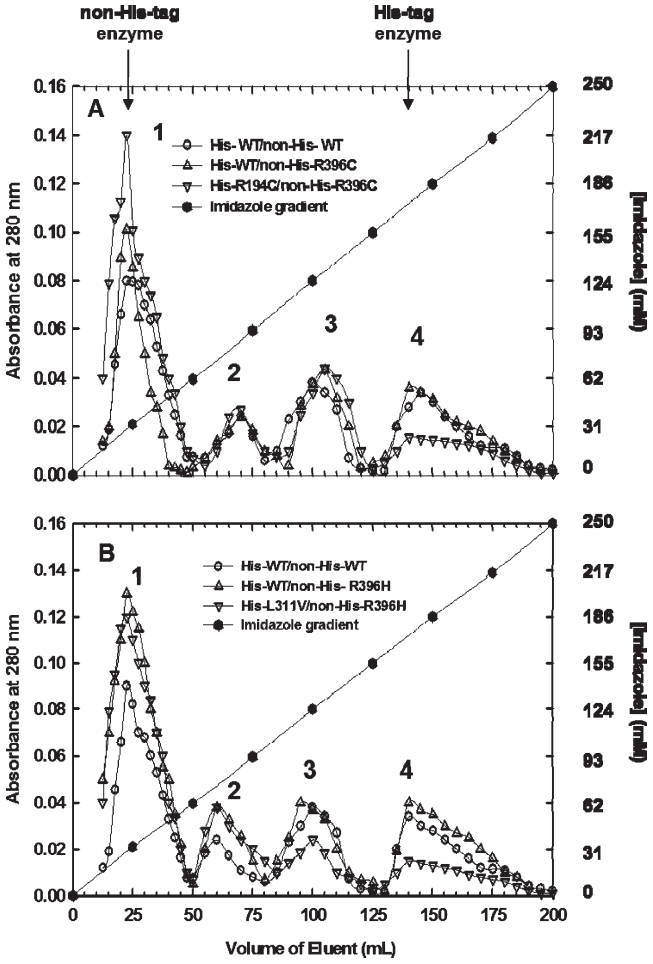

FIGURE 4: Elution profiles of the enzyme pairs treated with guanidine in the presence of the imidazole gradient. (A) Elution profiles related to the R194C/R396C pair. (B) Elution profiles related to the L311V/R396H pair. The fractions that had highest absorbance for elution of pure non-His-tagged WT and His-tagged WT are shown by two arrows atop the graph. The four peaks in each elution profile are numbered 1−4. The elution profile of the His-tagged WT/non-His-tagged WT pair is shown in both graphs. The volume of each fraction is 2.5 mL.

~33% of the protein recovered consists of hybrids. (Although the amount of hybrids formed under these in vitro conditions may not seem large compared with the amount of the original enzymes, the extent of dissociation of the ASL tetramer depends on the harshness of the conditions used for denaturation. We sought to optimize the solubility and preservation of activity while forming sufficient amounts of hybrids to allow their characterization.) N-Terminal sequencing of pools 2 and 3 of each enzyme pair indicates that each pool consists of His-tagged and non-His-tagged proteins, implying that hybrids are present. However, quantitative results of the precise ratios of the His-tagged and non-His-tagged proteins were hard to obtain because of the poor yield upon Edman sequencing of the six His residues in the His-tagged enzyme.

AUC Data of Hybrid Pools. To assess the molecular mass of each enzyme pool, we used analytical ultracentrifugation (AUC). We have previously shown that the ASLs exist as a mixture of species, e.g., monomer/tetramer, dimer/tetramer, trimer/tetramer, etc. (*5*, *26*). A constant concentration of ~0.1 mg/mL was used for all the enzymes, and the experimental AUC data at 25 °C were fitted to various theoretical models for a mixture of an oligomer with species with different molecular

Table 2: Molecular Mass Data of Hybrid Pools of Human ASL at 25 °C and pH 7.0

	molecular mass by AUC[a] (kDa)	
enzyme	M-Tet	D-Tet
His-tagged WT	58 ± 1 (23%)	
	228 ± 0.5 (77%)	
His-tagged R194C	57 ± 1 (27%)	
	229 ± 2 (73%)	
His-tagged L311V	57 ± 0.5 (32%)	
	230 ± 1 (68%)	
His-tagged R396H		116 ± 1 (20%)
		227 ± 2 (80%)
His-tagged R396C	56 ± 2 (22%)	
	227 ± 1 (78%)	
non-His-tagged WT/His-tagged WT		
pool 1	55 ± 0.8 (32%)	
	219 ± 1 (68%)	
pool 2[b]	56 ± 3 (27%)	
	223 ± 2 (73%)	
pool 3[b]	55 ± 2 (25%)	
	230 ± 2 (75%)	
non-His-tagged R396C/ His-tagged WT		
pool 1	55 ± 1 (24%)	
	218 ± 2 (76%)	
pool 2	56 ± 0.6 (27%)	
	222 ± 1 (72%)	
pool 3[c]	57 ± 1 (30%)	
	227 ± 3 (70%)	
non-His-tagged R396H/ His-tagged WT		
pool 1	54 ± 1 (25%)	
	221 ± 2 (75%)	
pool 2[d]	58 ± 1 (27%)	
	225 ± 2 (73%)	
pool 3	57 ± 1 (28%)	
	229 ± 2 (72%)	
non-His-tagged R396C/ His-tagged R194C		
pool 1	54 ± 1 (20%)	
	217 ± 3 (80%)	
pool 2[e]	57 ± 2 (22%)	
	223 ± 3 (78%)	
pool 3[e]	56 ± 2 (20%)	
	227 ± 2 (80%)	
non-His-tagged R396H/ His-tagged L311V		
pool 1	55 ± 0.5 (26%)	
	220 ± 2 (74%)	
pool 2[f]	57 ± 2 (26%)	
	224 ± 2 (74%)	
pool 3[f]	58 ± 3 (26%)	
	229 ± 2 (74%)	

[a]The molecular mass by AUC was measured at 25 °C, using an ~0.1 mg/mL sample in fresh enzyme storage buffer (pH 7.0) at 11000 rpm. The experiments were performed within 48 h of elution of all the pools. Abbreviations: M, monomer; D, dimer; Tri, trimer; Tet, tetramer; −, different species in equilibrium. The percentage of each species is given in parentheses. [b]AUC data for pools 2 and 3 of the non-His-tagged WT/His-tagged WT pair also fit to the D-Tet (27%, 73%) model. [c]AUC data for pool 3 of the non-His-tagged R396C/His-tagged WT pair also fit to the M-Tri (30%, 70%) model. [d]AUC data for pool 2 of the non-His-tagged R396H/His-tagged WT pair also fit to the M-5mer (29%, 71%) model. [e]AUC data for the non-His-tagged R396C/His-tagged R194C pair from pool 2 also fit to the M-5mer (25%, 75%) model, while AUC data for pool 3 also fit to the M-Tri (18%, 82%) model. [f]AUC data for pools 2 and 3 of the non-His-tagged R396H/His-tagged L311V pair also fit to the M-5mer (30%, 70%) model.

masses. Because the results at 280, 240, and 220 nm are similar, only the representative experimental data and residuals at 280 nm, which illustrate goodness of fit for various models [e.g., monomer/tetramer (M-Tet) or dimer/tetramer (D-Tet)], are shown in the Supporting Information (Figures 1S−3S). Results of the molecular mass analyses of pools 1−3 are summarized in Table 2. The subunit molecular masses of the pure non-His-tagged and His-tagged enzymes are ~55000 and ~57000 Da, respectively; therefore, a tetramer of the non-His-tagged enzyme would be expected to have a molecular mass of ~220000 Da, while a pure His-tagged enzyme would have a molecular mass of ~228000 Da. The five original purified His-tagged individual enzymes are shown at the top of Table 2 and exhibit tetramers of ~228 kDa.

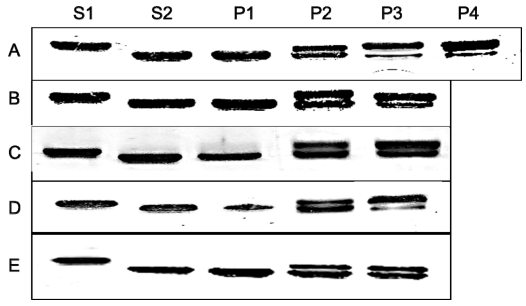

FIGURE 5: Representative SDS−PAGE gels of each enzyme pair. Standards 1 and 2 (S1 and S2, respectively) are His-tagged and non-His-tagged protein, respectively, of each pair. P1−P4 represent the pools in the elution profile of each pair. (A) Gel of the non-His-tagged WT/His-tagged WT pair. (B) Gel of the non-His-tagged R396C/His-tagged WT pair. (C) Gel of the non-His-tagged R396H/His-tagged WT pair. (D) Gel of the non-His-tagged R396C/His-tagged R194C pair. (E) Gel of the non-His-tagged R396H/His-tagged L311V pair. The band for the P4 pool from all the pairs is similar to that of the WT/WT pair and has been omitted from gels B−E for the sake of clarity.

According to the best fit models shown in Table 2, all the pools have predominant amounts of tetramer, indicating that the enzyme mixtures, which were initially denatured with guanidinium chloride, indeed renatured and reassociated when guanidinium chloride was removed. The AUC results indicate that the experimental AUC data of pools 1−4 of all the hybrid pairs have a good fit with the monomer/tetramer model. In some of the cases, the results can also be fit either to monomer/5mer models (Table 2), which may be indicative of some instability of the hybrids, or to the monomer/trimer model (Table 2), suggesting that there may be unfavorable interactions between the two types of enzyme subunits.

SDS−PAGE. Denaturing gels were used for evaluation of the approximate amounts of His-tagged and non-His-tagged protein in each pool, because a His-tagged subunit of ASL exhibits a molecular mass of ~57000 Da, whereas a non-His-tagged subunit of ASL has a molecular mass of ~55000 Da. These gels gave reproducible bands. Representative gels of each pair are shown in Figure 5. The subunit ratios estimated from these gels (represented as non-His-tagged:His-tagged ratios) are listed in Table 3 (column 2).

It is apparent from the SDS gels that, along the imidazole gradient, initially there is pure non-His-tagged protein (pool 1) followed by pool 2, which is a hybrid with either approximately equal amounts of non-His-tagged and His-tagged protein or more non-His-tagged protein than His-tagged protein. Pool 3 is also a hybrid and has more His-tagged protein (either double or triple the amount of non-His-tagged enzyme). Pool 4 contains predominantly His-tagged protein with a small amount of

Table 3: Subunit Ratios of the Enzyme from SDS−PAGE and Enzymatic Activities of the Heterotetramer at 25 °C

		enzymatic activity[a]			
		SAMP (% of WT)		SAICAR (% of WT)	
enzyme	subunit ratio (non-His-tagged:His-tagged)	E_{meas}	E_{calc}	E_{meas}	E_{calc}
WT		100		100	
R194C		125		107	
L311V	NA[b]	90	NA[b]	86	NA[b]
R396H		20		22	
R396C		21		29	
non-His-tagged WT/His-tagged WT					
pool 2	1.3:1	95	100	93	100
pool 3	1:3.7	95	100	93	100
non-His-tagged R396C/His-tagged WT					
pool 2	1.2:1	45	50	60	56
pool 3	1:2.3	100	76	82	79
non-His-tagged R396H/His-tagged WT					
pool 2	1.1:1	59	57	62	58
pool 3	1:1.6	102	68	85	69
non-His-tagged R396C/His-tagged R194C					
pool 2	1.2:1	65	68	64	65
pool 3	1:3.2	113	100	103	88
non-His-tagged R396H/His-tagged L311V					
pool 2	1.8:1	57	44	56	45
pool 3	1:1	85	56	80	54

[a]The activity of each pool for SAMP and SAICAR was measured separately at 25 °C by addition of a 10 μL aliquot of enzyme to 1.0 mL of a solution containing 50 mM HEPES buffer (pH 7.4) and each substrate at 60 μM. E_{calc} is the calculated specific activity of each pool relative to that of WT, and E_{meas} is the measured specific activity relative to that of WT. The specific activities of the WT enzyme with respect to SAMP and SAICAR are 9.2 and 15 μmol min^{-1} mg^{-1}, respectively. [b]Not applicable.

Table 4: Inactivation Rate Constants of Pure Human ASL Enzymes and Pool 2 of the Hybrid Pairs at 60 °C[a]

enzyme	k_i (h^{-1})[b]
His-tagged WT	0.086 ± 0.004
His-tagged L311V	0.059 ± 0.005
His-tagged R396H	0.096 ± 0.007
His-tagged R396C	0.103 ± 0.01
His-tagged R194C	2.76 ± 0.1
pool 2 of the non-His-tagged R396C/His-tagged R194C pair	0.255 ± 0.02
pool 2 of the non-His-tagged WT/His-tagged WT pair	0.099 ± 0.003
pool 2 of the non-His-tagged R396H/His-tagged WT pair	0.101 ± 0.007
pool 2 of the non-His-tagged R396H/His-tagged L311V pair	0.122 ± 0.003

[a]The enzyme samples (0.2 mg/mL) in fresh enzyme storage buffer (pH 7.0) were incubated at 60 °C. Aliquots were removed periodically, and the activity was measured at 25 °C by addition of a 10 μL aliquot of enzyme to 1.0 mL of a solution containing 50 mM HEPES buffer (pH 7.4) and each substrate at 60 μM (SAMP). [b]The k_i value for each reaction was determined from the slope of $\ln(E_t/E_0)$ vs time. E_t and E_0 are the specific activity at time t and time zero, respectively. The values are shown along with their standard errors.

non-His-tagged protein. The gel pattern of pool 4 of the WT/mutant and mutant/mutant pairs was similar to that of the WT/WT pair. Polyacrylamide gels run under conditions that maintained the enzyme in its native state (i.e., no SDS) have also demonstrated the existence of several bands in pools 2 and 3. However, these gels were more difficult to quantify.

SAMP and SAICAR Activity of the Hybrid Pools. The two substrates for ASL are SAMP and SAICAR. Therefore, we sought to evaluate separately the activity of the hybrid enzyme pools with each of the two substrates under saturating conditions (60 μM substrate) at pH 7.4 in the direction of fumarate formation. The E_{meas} (measured specific activity relative to that of WT) and E_{calc} (calculated specific activity relative to that of WT) values for each pool of the enzyme pairs are summarized in Table 3. The expected activity of each hybrid pool was calculated using the subunit ratios obtained by SDS−PAGE and the V_{max} values of the homotetramers (Table 5).

If the subunits of the heterotetramer act independently, E_{meas} should be similar to E_{calc}. The E_{meas} values for SAMP and SAICAR of pool 2 are similar to the E_{calc} values of the respective pairs, implying that there is little or no influence from one type of subunit on the other when there are equal amounts of the non-His-tagged enzyme (in these cases, the less active enzyme) and His-tagged enzyme (in these cases, the more active enzyme). However, the E_{meas} values for SAMP and SAICAR of pool 3 of the respective pairs are greater than the corresponding E_{calc} values, indicating that when the His-tagged enzyme is predominant, it influences the activity of the mutant subunit with a lower activity.

Thermal Stability at 60 °C. Because we have studied the stability of each individual enzyme under the relatively harsh conditions at 60 °C (*5*), we sought to evaluate the stability of the hybrids under the same conditions. The time-dependent inactivation plots are illustrated in Figure 6. The inactivation rate constant (k_i) value for pool 2 of each enzyme pair was determined from the slope of $\ln(E_t/E_0)$ versus time, and the data are summarized in Table 4.

It is evident that multiple types of pool 2 (with approximately equal amounts of non-His-tagged and His-tagged or more non-His-tagged enzyme subunits) are relatively stable under the harsh conditions at 60 °C and no insoluble aggregate formation was observed. There is a significant increase in the stability of pool 2 of the non-His-tagged R396C/His-tagged R194C pair as compared to that of His-tagged R194C (Figure 6B); this is shown by the 10-fold lower inactivation rate constant for the hybrid non-His-tagged R396C/His-tagged R194C pair as compared to that of homotetrameric R194C (Table 4).

Kinetics of Hybrid Pools. All the pools of each enzyme pair were characterized kinetically using SAMP. The kinetic data were analyzed using the Hill equation, and representative plots of velocity versus SAMP concentration from each enzyme pair are shown in the Supporting Information (Figures 4S and 5S). The data at pH 7.4 in the direction of AMP formation for pools 1−3 in each enzyme pair are summarized in Table 5.

The kinetic data of pool 1 of each enzyme pair are similar to those of the corresponding non-His-tagged enzyme, indicating that pool 1 contains pure non-His-tagged enzyme. All the pools of the His-tagged WT/non-His-tagged WT enzyme pair have kinetic parameters similar to that of the pure WT. Furthermore, the pools have a Hill coefficient of 1.8, indicating that there is positive cooperativity. In contrast, pool 2 of WT/mutant and mutant/mutant enzyme pairs has an intermediate V_{max} (average of the two pure enzymes), while the V_{max} of pool 3 is similar to that of the corresponding His-tagged enzyme. There is minimal change in the $K_{0.5}$ values in pools 2 and 3 of all the enzyme pairs, indicating that hybridization has a weaker effect on substrate affinity. The Hill coefficients of pools 2 and 3 of WT/mutant pairs are ∼1.5, suggesting that the positive cooperativity is slightly reduced compared to that of the pure WT enzyme.

DISCUSSION

Human adenylosuccinate lyase deficiency is a metabolic disorder that is caused by mutations to the ASL gene, most of which are missense mutations. Furthermore, the majority of these missense mutations occur far from the active site. Because many ASL deficient human patients are compound heterozygotes, the existence of various hybrids has been hypothesized. In this study, we evaluated the feasibility of in vitro hybridization and separation of different hybrid mixtures followed by characterization of the hybrid pools. For this study, we chose the R194C/R396C and L311V/R396H mutant pairs. We also used the WT/R396C and WT/R396H pairs to mimic the situation of parents of ASL deficient patients. As a control, we performed hybridization using His-tagged WT and non-His-tagged WT. Because ASL is a tetramer, mixing of two types of mutant enzymes can produce three different types of hybrid tetramers with non-His-tagged:His-tagged ratios of 3:1, 2:2, and 1:3.

The elution profiles of the WT/WT pair and the other enzyme pairs indicate that hybrids have formed, and for the first time, we have been successful in separating the hybrids. Previously, it has been shown that hybrids of ASL are formed when two different types of mutant enzymes are coexpressed, but the authors did not separate the various hybrids (*27*). It is evident from the SDS−PAGE results that pools 2 and 3 of all the enzyme pairs contain hybrids.

The subunit ratio of pool 2 is approximately 1:1 (non-His-tagged:His-tagged) in most cases. For each substrate, the measured activity (E_{meas}) of pool 2 of all the enzyme pairs approximates the average of the corresponding activities of the two enzymes in the respective pair. Because each active site of ASL is formed from different regions of three subunits (Figure 2, I), two

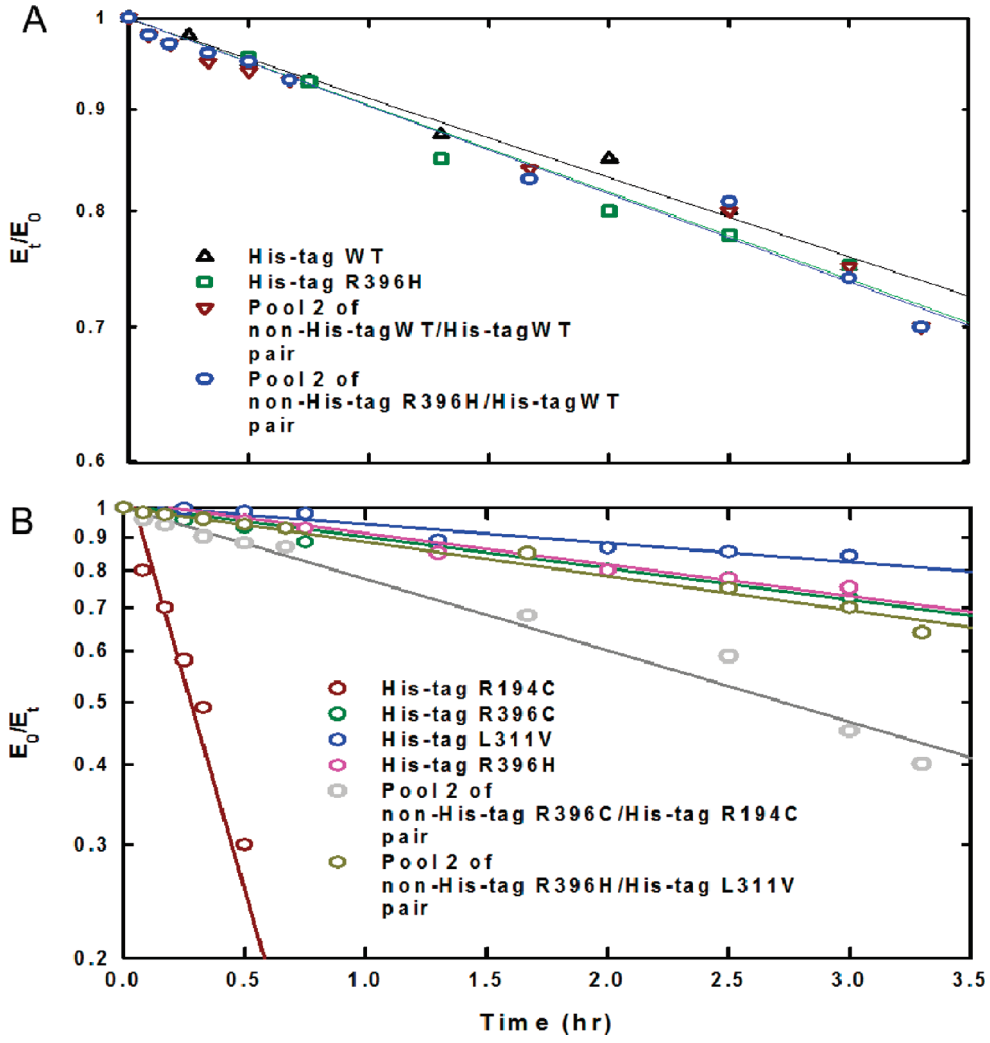

FIGURE 6: Time-dependent thermal inactivation plots of the individual His-tagged enzymes and pool 2 of the enzyme pairs at 60 °C. (A) Ln(E_t/E_0) vs time plots of His-tagged WT, His-tagged R396H, and pool 2 of the non-His-tagged WT/His-tagged WT pair and the non-His-tagged R396H/His-tagged WT pair. (B) Ln(E_t/E_0) vs time plots of His-tagged R194C, His-tagged R396C, His-tagged L311V, His-tagged R396H, and pool 2 of the non-His-tagged R396C/His-tagged R194C pair and the non-His-tagged R396H/His-tagged R396H pair. E_t is the specific activity at time t, and E_0 is the specific activity at time zero.

active sites of the tetramer of pool 2 have more contributions from the subunits of the less active mutant whereas the other two active sites make have more contributions from the more highly active enzyme (either WT or mutant). This leads to a 50% contribution from each type of subunit to the overall activity. Although for each substrate the measured activity (E_{meas}) of pool 2 of all the enzyme pairs is similar to the respective E_{calc} values, the kinetic data reveal that the types of pool 2 of all the pairs have different degrees of positive cooperativity (Table 5), suggesting that there may be very weak positive cooperativity among the subunits. On the other hand, as the amount of His-tagged protein increases, as in pool 3, for each active site of the tetramer there is a greater contribution from the His-tagged protein with the higher activity leading to an increase in activity (Tables 3 and 5). Furthermore, the E_{meas} values of pool 3 of all the enzyme pairs are higher than the corresponding E_{calc} values, suggesting that the subunits may have some influence on each other. It is apparent from the kinetic data that pool 3 of all the pairs retains the positive cooperativity of the corresponding His-tagged enzyme (Table 5). This observation suggests that there is a disproportionately strong influence on the overall activity from the more active His-tagged enzyme.

An important observation is that similar differences between E_{meas} and E_{calc} were obtained regardless of the substrate used (either SAMP or SAICAR). This result is consistent with the active site being the same for both substrates (*18*, *28*). Similar results have been reported in an independent study of disease-associated human ASL mutants (*27*). It has been suggested that the different levels of the two dephosphorylated substrates detected in some ASL-deficient patients are not due to the enzyme having two different active sites for the two substrates; instead, they may be due to either unequal rates of dephosphorylation of the two substrates or different transport rates of the two dephosphorylated substrates out of the cell (*18*).

Previously, it was shown that the R194C mutant enzyme is the most unstable mutant under harsh conditions (e.g., at 60 °C) because of the rapid oxidation of its cysteines (*5*). In contrast, the other mutant enzymes were stable for ~2−3 h, after which some insoluble aggregates were observed. Notably, we have now found that the R396C/R194C hybrid pool 2 enzyme is 10 times more stable than the pure R194C mutant enzyme (Table 4). Clearly, interactions of the less active R396C subunits with the R194C subunits have stabilized the mutants in the hybrid, although this hybrid is still less stable than the WT enzyme. Hybrid pool 2 of

Table 5: Kinetic Parameters of Human ASL Hybrid Pairs at 25 °C

enzyme	V_{max}[a] (μmol min^{-1} mg^{-1})	$K_{0.5}$[a] (μM)	Hill coefficient[a]
WT	9.2 ± 0.1	1.9 ± 0.05	1.8 ± 0.1
R194C	12.0 ± 0.9	2.2 ± 0.3	1.3 ± 0.2
L311V	8.6 ± 0.7	3.4 ± 0.5	1.3 ± 0.1
R396H	1.9 ± 0.2	3.8 ± 0.8	0.9 ± 0.2
R396C	2.0 ± 0.2	1.1 ± 0.2	0.9 ± 0.1
non-His-tagged WT/His-tagged WT pair	9.8 ± 0.3	2.2 ± 0.1	1.8 ± 0.2
non-His-tagged R396C/His-tagged WT pair			
pool 1	2.1 ± 0.3	1.0 ± 0.1	1.0 ± 0.1
pool 2	4.2 ± 0.1	1.1 ± 0.1	1.4 ± 0.2
pool 3	9.2 ± 0.7	3.2 ± 0.3	1.6 ± 0.1
non-His-tagged R396H/His-tagged WT pair			
pool 1	1.9 ± 0.1	3.2 ± 0.9	0.7 ± 0.06
pool 2	5.5 ± 0.2	1.9 ± 0.2	1.4 ± 0.1
pool 3	9.4 ± 0.6	2.7 ± 0.3	1.5 ± 0.2
non-His-tagged R396C/His-tagged R194C pair			
pool 1	2.2 ± 0.1	1.3 ± 0.3	0.8 ± 0.1
pool 2	6.0 ± 0.2	1.9 ± 0.2	1.5 ± 0.2
pool 3	10.4 ± 0.4	1.9 ± 0.2	1.2 ± 0.1
non-His-tagged R396H/His-tagged L311V pair			
pool 1	1.9 ± 0.1	3.2 ± 0.9	0.7 ± 0.06
pool 2	5.3 ± 0.2	1.0 ± 0.1	1.2 ± 0.1
pool 3	7.9 ± 0.6	2.4 ± 0.4	1.1 ± 0.1

[a]The V_{max}, $K_{0.5}$, and Hill coefficient values were determined by varying the concentration of SAMP and fitting the data to the Hill equation using SigmaPlot. The values of V_{max} and $K_{0.5}$ are shown along with their standard errors.

the R396C/R194C pair is also less stable than that of the R396H/L311V pair under harsh conditions at 60 °C. These results suggest that under in vivo conditions of ASL deficient patients, it may be possible that the patient with the R194C/R396C mutant pair produces relatively unstable hybrid and nonhybrid mixtures leading to a severe form of ASL deficiency that presents as only a neonatal form. On the other hand, the patient with the L311V/R396H mutant pair may produce more stable hybrid and nonhybrid mixtures leading to ASL deficiency that presents as the childhood severe form. Apparently, there are favorable interactions between the subunits of WT and mutant enzymes, which can lead to the formation of more active and stable hybrid mixtures. This may account for the parents of ASL deficient patients being normal.

The other characteristic of the ASL deficient patients is the presence of larger amounts of dephosphorylated substrates in cerebrospinal fluid than in urine and the development of mental retardation. Adenylosuccinate lyase participates in two pathways: the de novo purine biosynthesis pathway and the purine nucleotide cycle. Both pathways are active during development and throughout life (*29*, *30*). However, the demand for purines during development and throughout life is different. Therefore, the two pathways are tightly regulated in distinct ways to meet the demand. It has been shown that all six enzymes in the de novo purine biosynthesis pathway colocalize to form the "purinosome" during purine biosynthesis to channel each product for the next step (*31*). Mutant enzymes of purine biosynthesis may affect the stability of the purinosome to different extents. Furthermore, different downstream intermediates regulate both pathways; for example, an increase in SAICAR levels upregulates the gene expression of de novo purine synthesis (*32*−*34*). During the developmental stage, there is a strong demand for purines and the de novo purine biosynthesis pathway is more highly active than the purine nucleotide cycle (*35*). Furthermore, purine nucleotides are particularly important as modulators of neurotransmitters and regulators of the synaptic availability of neurotransmitters (*36*). It may be postulated that more profound brain damage could result in newborns and present as the neonatal fatal form of ASL deficiency due to accumulation of more SAICAR (with its greater toxicity) than SAMP. However, after birth, both pathways become equally active to meet the purine demand. In ASL deficient patients, this would lead to accumulation of both substrates, SAMP and SAICAR, at similar or slightly different levels, particularly in the cerebrospinal fluid, which may result in slow progression of brain damage. Therefore, in such newborns, ASL deficiency presents as the severe childhood form that progresses slowly with age and ultimately results in severe mental retardation.

In conclusion, we have shown that in vitro hybridization of two different enzymes is possible under reversibly denaturing conditions, and we were successful in separating various hybrids. The molecular mass data indicate that different types of subunits reassociated to form predominant amounts of heterotetramers and that the extent of favorable interactions between different types of subunits depends upon the mutant enzyme. We have shown that the hybrids are relatively stable under harsh conditions at 60 °C and that the hybrids have positive cooperativity to different degrees. Our results indicate that formation of hybrids is advantageous to ASL deficient patients as well as their parents. However, under in vivo conditions, the formation of hybrids may not be sufficiently effective to prevent symptoms of ASL deficiency disease.

ACKNOWLEDGMENT

We thank Dr. Yu-Chu Huang for N-terminal sequencing and Mr. John Dykins for running the mass spectrometer.

SUPPORTING INFORMATION AVAILABLE

Experimental AUC data were fitted to various theoretical models for an oligomer in equilibrium with species of different molecular masses. Representative experimental data and residuals, which illustrate the goodness of fit for hybrid pools 2 and 3

of each enzyme pair, are shown in Figures 1S−3S. Representative kinetic plots of specific activity (v) versus SAMP concentration for each enzyme pair are shown in Figures 4S and 5S. This material is available free of charge via the Internet at http://pubs.acs.org.

REFERENCES

1. Ratner, S. (1972) Argininosuccinases and adenylosuccinases. In The Enzymes (Boyer, P. D., Ed.) 3rd ed., Vol. 7, pp 167−197, Academic Press, New York.
2. Mouchegh, K., Zikanova, M., Hoffmann, G. F., Kretzschmar, B., Kuhn, T., Mildenberger, E., Stoltenburg-Didinger, G., Krijt, J., Dvorakova, L., Honzik, T., Zeman, J., Kmoch, S., and Rossi, R. (2007) Lethal fetal and early neonatal presentation of adenylosuccinate lyase deficiency: Observation of 6 Patients in 4 Families. *J. Pediatr. 150*, 57–61.
3. Jaeken, J., and Van den Berghe, G. (1984) An infantile autistic syndrome characterized by the presence of succinylpurines in body fluids. *Lancet II*, 1058–1061.
4. Jaeken, J., Wadman, S. K., Duran, M., Van Sprang, F. J., Beemer, F. A., Holl, R. A., Theunissen, P. M., de Cock, P., Van den Bergh, F., Vincent, M. F., and Van den Berghe, G. (1988) Adenylosuccinase deficiency: An inborn error of purine nucleotide synthesis. *Eur. J. Pediatr. 148*, 126–131.
5. De Zoysa Ariyananda, L., Lee, P., Antonopoulos, C., and Colman, R. F. (2009) Biochemical and biophysical analysis of five disease-associated human adenylosuccinate lyase mutants. *Biochemistry 48*, 5291–5302.
6. Speigel, E. K., Colman, R. F., and Patterson, D. (2006) Adenylosuccinate lyase deficiency. *Mol. Genet. Metab. 89*, 19–31.
7. Van den Berghe, G., and Jaeken, J. (2001) Adenylosuccinate lyase deficiency. In The Metabolic and Molecular Basis of Inherited Diseases (Scriver, C. R., Beaudt, A. L., Valle, D., Sly, W. S., Childs, B., Kinzler, K. W., and Vogelstein, B., Eds.) 8th ed., Vol. II, pp 2653−2662, McGraw-Hill, New York.
8. Castro, M., Perez-Cerda, C., Merinero, B., Garcia, M. J., Bernar, J., Gil Nagel, A., Torres, J., Bermudez, M., Garavito, P., Marie, S., Vincent, F., Van den Berghe, G., and Ugarte, M. (2002) Screening for adenylosuccinate lyase deficiency: Clinical, biochemical and molecular findings in four patients. *Neuropediatrics 33*, 186–189.
9. Brosius, J. L., and Colman, R. F. (2002) Three subunits contribute amino acids to the active site of tetrameric adenylosuccinate lyase: Lys268 and Glu275 are required. *Biochemistry 41*, 2217–2226.
10. Lee, T. T., Worby, C., Bao, Z., Dixon, J. E., and Colman, R. F. (1999) His68 and His141 are critical contributors to the intersubunit catalytic site of adenylosuccinate lyase of *Bacillus subtilis*. *Biochemistry 38*, 22–32.
11. Segall, M. L., and Colman, R. F. (2004) Gln212, Asn270, and Arg301 are critical for catalysis by adenylosuccinate lyase from *Bacillus subtilis*. *Biochemistry 43*, 7391–7402.
12. Segall, M. L., Cashman, A. A., and Colman, R. F. (2007) Important roles of hydroxylic amino acid residues in the function of *Bacillus subtilis* adenylosuccinate lyase. *Protein Sci. 16*, 441–448.
13. Antonopoulos, C. H., De Zoysa Ariyananda, L., Lee, P., Currier, J. M., and Colman, R. F. (2009) Experimental Biology, Abstract 504.4.
14. Stenmark, P., Moche, M., Arrowsmith, C., Berglund, H., Busam, R., Collines, R., Dahlgren, L. G., Edwards, A., Flodin, S., Flores, A., et al. (2010) Human adenylosuccinate lyase in complex with its substrate N6-(1,2-dicarboxy-ethyl)-AMP, and its products AMP and fumarate. RCSB Protein Data Bank entry 2VD6.
15. Sivendran, S., Patterson, D., Spiegel, E., McGown, I., Cowley, D., and Colman, R. F. (2004) Two novel mutant human adenylosuccinate lyases (ASLs) associated with autism and characterization of the equivalent mutant *Bacillus subtilis* ASL. *J. Biol. Chem. 279*, 53789–53797.
16. Lee, P., and Colman, R. F. (2007) Expression, purification, and characterization of stable, recombinant human adenylosuccinate lyase. *Protein Expression Purif. 51*, 227–234.
17. Laemmli, U. K. (1970) Cleavage of structural protein during the assembly of the head of bacteriophage T4. *Nature 227*, 680–685.
18. Sivendran, S., and Colman, R. F. (2008) Effect of a new non-cleavable substrate analog on wild-type and serine mutants in the signature sequence of adenylosuccinate lyase of *Bacillus subtilis* and *Homo sapiens*. *Protein Sci. 17*, 1162–1174.
19. Palenchar, J. B., and Colman, R. F. (2003) Characterization of a mutant *Bacillus subtilis* adenylosuccinate lyase equivalent to a mutant enzyme found in human adenylosuccinate lyase deficiency: Asparagine 276 plays an important structural role. *Biochemistry 42*, 1831–1841.
20. Tornheim, K., and Lowenstein, J. M. (1972) The purine nucleotide cycle: The production of ammonia from aspartate by extracts of rat skeletal muscle. *J. Biol. Chem. 247*, 162–169.
21. Woodward, D. O., and Bramer, H. D. (1966) Purification and properties of *Neurospora* adenylosuccinase. *J. Biol. Chem. 241*, 580–586.
22. Image processing and analysis using ImageJ (http://rsbweb.nih.gov/ij).
23. Hearne, J. L., and Colman, R. F. (2006) Catalytically active monomer of class Mu glutathione transferase from rat. *Biochemistry 45*, 5974–5984.
24. SEDPHAT (http://www.analyticalultracentrifugation.com/sedphat/sedphat.htm).
25. Laue, T. M., Shah, B. D., Ridgeway, T. M., and Pelletier, S. L. (1992) Computer-aided interpretation of analytical sedimentation data for proteins. Analytical Ultracentrifugation in Biochemistry and Polymer Science (Harding, S. E., Rowe, A., and Horton, J. C., Eds.) pp 90−125, Royal Society of Chemistry, Cambridge, U.K.
26. De Zoysa Ariyananda, L., and Colman, R. F. (2008) Evaluation of types of interactions in subunit association in *Bacillus subtilis* adenylosuccinate lyase. *Biochemistry 47*, 2923–2934.
27. Zikanova, M., Skopova, V., Hnizda, A., Krijt, J., and Kmoch, S. (2010) Biochemical and structural analysis of 14 mutant ADSL enzyme complexes and correlation to phenotypic heterogeneity of adenylosuccinate lyase deficiency. *Hum. Mutat. 31*, 445–455.
28. Stone, R. L., Zalkin, H., and Dixon, J. E. (1997) Expression, purification and kinetic characterization of recombinant human adenylosuccinate lyase. *J. Biol. Chem. 268*, 19710–19716.
29. Flanagan, W. F., Holmes, E. W., Sabina, R. L., and Swain, J. L. (1986) Importance of purine nucleotide cycle to energy production in skeletal muscles. *Am. J. Physiol. 251* (5, Part 1), C795–C802.
30. Van den Berghe, G., Bontemps, F., Vincent, M. F., and Van den Bergh, F. (1992) The purine nucleotide cycle and its metabolic defects. *Prog. Neurobiol. 39*, 547–561.
31. An, S., Kumar, R., Sheets, E. D., and Benkovic, S. J. (2008) Reversible compartmentalization of de novo purine biosynthetic complexes in living cells. *Science 320*, 103–106.
32. Pinson, B., Vaur, S., Sagot, I., Coulpier, F., Lemoine, S., and Daidnan-Fornier, B. (2009) Metabolic intermediates selectively stimulate transcriptional factor interaction and modulate phosphate and purine pathways. *Genes Dev. 23*, 1399–1407.
33. Rébora, K., Desmoucelles, C., Borne, F., Pinson, B., and Daignan-Fornier, B. (2001) Yeast AMP pathway genes respond to adenine through regulated synthesis of a metabolic intermediate. *Cell Biol. 21*, 7901–7912.
34. Rébora, K., Laloo, B., and Daignan-Fornier, B. (2005) Revisiting purine-histidine cross-pathway regulation in *Saccharomyces cerevisiae*: A central role for a small molecule. *Genetics 170*, 61–70.
35. Alexiou, M., and Leese, H. J. (1992) Purine utilization, de novo synthesis and degradation in mouse preimplantation embryos. *Development 114*, 185–192.
36. Deutsch, S. I., Long, K. D., Rosse, R. B., Mastropaolo, J., and Eller, J. (2005) Hypothesized deficiency of guanine-based purines may contribute to abnormalities of neurotransmission in Lesch-Nyhan Syndrome. *Clin. Neuropharmacol. 28*, 28–37.